OPEN

NPG Asia Materials (2016) 8, e251; doi:10.1038/am.2016.17
www.nature.com/am

ORIGINAL ARTICLE

The relationship between magneto-optical properties and molecular chirality

Satoshi Wada[1], Yuichi Kitagawa[2], Takayuki Nakanishi[2], Koji Fushimi[2], Yasuhiro Morisaki[3,4], Koji Fujita[3], Katsuaki Konishi[5], Katsuhisa Tanaka[3], Yoshiki Chujo[3] and Yasuchika Hasegawa[2]

The chiral nonanuclear Tb(III) clusters $[Tb_9(sal\text{-}(R)\text{-}Bt)_{16}(\mu\text{-}OH)_{10}]^+[NO_3]^-$ (Tb-(*R*)-Bt: sal-(*R*)-Bt = (*R*)-2-butyl salicylate) and $[Tb_9(sal\text{-}(S)\text{-}Bt)_{16}(\mu\text{-}OH)_{10}]^+[NO_3]^-$ (Tb-(*S*)-Bt: sal-(*S*)-Bt = (*S*)-2-butyl salicylate) were found to exhibit a unique magneto-optical property: the Faraday effect. The clusters were composed of 9 Tb(III) ions bridged by 10 μ-OHs and 16 chiral salicylic acid esters. The Faraday rotation angle of Tb-(*R*)-Bt was greater than that of Tb-(*S*)-Bt, indicating that the Faraday effect was affected by the chirality of the Tb(III) clusters. The chiroptical properties of the Tb(III) clusters were estimated using circular dichroism and circularly polarized luminescence. In this study, a new finding concerning chiral magneto-optical properties was investigated.

NPG Asia Materials (2016) **8,** e251; doi:10.1038/am.2016.17; published online 25 March 2016

INTRODUCTION

The Faraday effect, a magneto-optical property, has received significant attention with regard to applications of magneto-optical materials. This effect causes the rotation of polarization by a material as the result of the application of an external magnetic field.[1] The degree of rotation is linearly proportional to the component of the magnetic field in the direction of propagation. The Faraday effect originates from the Zeeman splitting of electronic states based on the angular momentum of electrons in the material. Inorganic lanthanide compounds such as Tb(III)-doped borosilicate glasses and Tb(III) garnet ceramics exhibit large Faraday effects because of the large angular momentum of the 4f electron, and such materials have been used to construct optical isolators employed in optical communication systems.[2–5]

We recently described nonanuclear Tb(III) clusters coordinated with salicylate ligands that are a new type of lanthanide material exhibiting a large Faraday effect.[6] These clusters are composed of 9 Tb (III) ions bridged by 10 μ-OHs and 16 salicylic acid esters as organic ligands. The Faraday rotation angles of the clusters in the visible region are much larger than those of Tb glasses. We expect the clusters to be applied to next-generation optical communication systems. We also identified a further unique property of these clusters: the rotation angles were different depending on the organic ligands. This finding has the possibility to lead to new molecular designs for Faraday effect materials based on the type of the organic ligands.

In the present study, we focused on introducing chiral ligands to the Tb(III) cluster to maximize the unique characteristics of these inorganic–organic hybrid complexes. Lanthanide complexes containing chiral ligands show significant circular dichroism (CD) and circularly polarized luminescence (CPL) resulting from the differing absorption or luminescent intensities between left- and right-handed circularly polarized light.[7] These phenomena are derived from the chirality of the complexes; thus, their origin is markedly different from that of the Faraday effect.[1,8] The dissymmetry factors g_{CD} and g_{CPL} represent the magnitudes of the CD and CPL intensities, respectively, and the g_{CD} and g_{CPL} of the chiral lanthanide complexes are several hundred times larger than those of typical chiral organic molecules.[8–22] These larger dissymmetry factors are attributed to the large transition magnetic dipole moment of the lanthanide ion that shows opposing vectors depending on chirality. This moment is based on the angular momentum of electrons accompanying 4f–4f transitions. In CD and CPL studies, Richardson[9] established selection rules based on the *S*, *L* and *J* angular momentum quantum numbers of lanthanide 4f electron states, both experimentally and theoretically. Based on these rules, Muller and colleagues[13] reported the largest g_{CPL} value (>1.0) for a Eu(III) complex with chiral camphor-derivative ligands. As a general trend, Tb(III) complexes are also classified into a group having a large g_{CPL} among the lanthanide complexes,[22] expecting the large transition magnetic dipole moments of several transitions in the Tb(III) clusters.

For the first time, in this work, we introduced chiral ligands into Tb (III) clusters to investigate the effect of large transition magnetic dipole moments on the Faraday rotation. The chiral Tb(III) clusters $[Tb_9(sal\text{-}(R)\text{-}Bt)_{16}(\mu\text{-}OH)_{10}]^+[NO_3]^-$ (Tb-(*R*)-Bt: sal-(*R*)-Bt = (*R*)-2-butyl

[1]Graduate School of Chemical Sciences and Engineering, Hokkaido University, Hokkaido, Japan; [2]Faculty of Engineering, Hokkaido University, Hokkaido, Japan; [3]Graduate School of Engineering, Kyoto University, Kyoto, Japan; [4]School of Science and Technology, Kwansei Gakuin University, Hyogo, Japan and [5]Faculty of Environmental Earth Science and Graduate School of Environmental Science, Hokkaido University, Hokkaido, Japan
Correspondence: Professor Y Hasegawa, Faculty of Engineering, Hokkaido University, N13 W8, Kita-ku, Sapporo, Hokkaido 060-8628, Japan.
E-mail: hasegaway@eng.hokudai.ac.jp
Revised 23 October 2015; revised 11 December 2015; accepted 6 January 2016

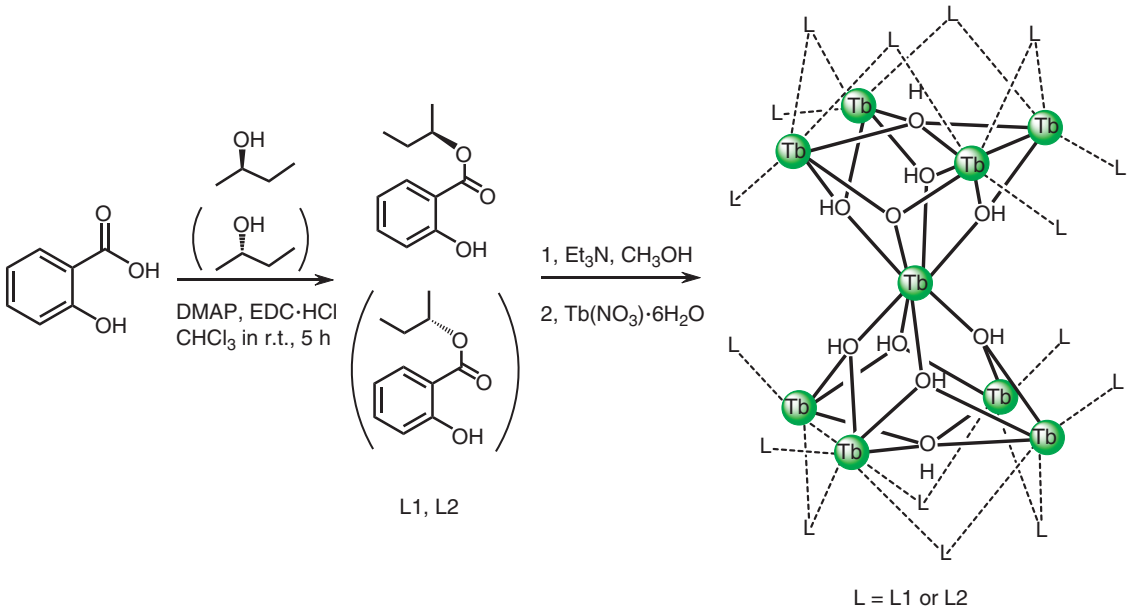

Figure 1 Synthetic scheme of a 2-butyl salicylate ligand and a nonanuclear Tb(III) cluster.

salicylate) and $[Tb_9(sal\text{-}(S)\text{-}Bt)_{16}(\mu\text{-}OH)_{10}]^+[NO_3]^-$ (Tb-(*S*)-Bt: sal-(*S*)-Bt = (*S*)-2-butyl salicylate) were synthesized by the complexation of $Tb(NO_3)\cdot 6H_2O$ with chiral organic ligands in methanol (CH_3OH) at 40 °C (Figure 1). The structures and chiroptical properties of these clusters were characterized using X-ray diffraction, CD and CPL measurements. We also performed Faraday effect measurements for these chiral Tb(III) clusters in poly(methyl methacrylate) (PMMA) films. The results showed that the Faraday rotation angles of these clusters were affected by their chirality. This study is the first report of a relationship between the Faraday effect and molecular chirality, providing new insights into the design of magneto-optical materials and also potentially opening up a novel field of chiral science.

MATERIALS AND METHODS

Materials

Salicylic acid ($C_6H_4(OH)COOH$), *N,N*-dimethyl-4-aminopyridine (DMAP, $C_7H_{10}N_2$), PMMA ($(C_5H_8O_2)_n$, Lot PDF4279), CH_3OH, and chloroform ($CHCl_3$) were purchased from Wako Pure Chemical Industries, Ltd (Osaka, Japan). (*R*)-(−)-2-butanol (C_4H_9OH, >99.0%), (*S*)-(+)-2-butanol (C_4H_9OH, >98.0%) and 1-ethyl-3-(3-dimethylaminopropyl) carbodiimide hydrochloride (EDC·HCl, $C_8H_{17}N_3\cdot HCl$) were purchased from Tokyo Chemical Industry Co., Ltd (Tokyo, Japan). Terbium(III) nitrate hexahydrate ($Tb(NO_3)_3\cdot 6H_2O$) and triethylamine (Et_3N, $(C_2H_5)_3N$) were purchased from Kanto Chemical Co., Inc (Tokyo, Japan).

Apparatus

Proton nuclear magnetic resonance (^{1}H-NMR) spectra were recorded in $CDCl_3$ on an auto-NMR JEOL ECS 400 MHz spectrometer (JEOL, Tokyo, Japan); $CHCl_3$ (δ_H = 7.26 p.p.m.) was used as an internal reference. Fast atom bombardment–mass spectrometry was performed using a JEOL JMS-700TZ spectrometer. Elemental analyses were performed using a J-SCIENCE MICRO CORDER JM10 system (Kyoto, Japan). Infrared spectra were recorded on a JASCO FT/IR-350 spectrometer (Tokyo, Japan). X-ray diffraction data were obtained using a RIGAKU SmartLab X-ray diffractometer (Tokyo, Japan). Photoluminescence (PL) spectra were measured using a Horiba FluoroLog3 spectrofluorometer (Kyoto, Japan, excitation wavelength = 380 nm). Luminescence quantum yields were measured using an JASCO FP-6300 spectrofluorometer with an integration sphere. The luminescence lifetimes were measured using the third harmonic (355 nm) of a Qswitched Nd:YAG laser. The electronic absorption, CD and CPL spectra were measured using a JASCO V-670 spectrophotometer, JASCO J-720 spectropolarimeter and JASCO CPL-200 spectrofluoropolarimeter (excitation wavelength = 380 nm), respectively. The quantitative elemental analyses were performed using an inductively coupled plasma atomic emission spectroscopy (ICP-AES, SHIMADZU ICPE-9000, Kyoto, Japan) to determine the concentration of the Tb(III) ion in PMMA films for the Faraday rotation measurements. The Faraday effect measurements were performed using a JASCO Model K-250 spectrophotometer.

Synthesis of (*R/S*)-2-butyl salicylate [Sal-(*R/S*)-Bt]

Salicylic acid (2.0 g, 14.5 mmol), (*R/S*)-(−/+)-2-butanol (1.08 g, 14.5 mmol), EDC·HCl (2.78 g, 14.5 mmol) and DMAP (0.177 g, 1.45 mmol) were added to $CHCl_3$ (40 ml). The mixture was stirred at room temperature for 5 h under Ar, washed with HCl aq. (2×30 ml) and $NaHCO_3$ aq. (2×30 ml) and distilled H_2O (2×30 ml). The organic layer was separated and dried with $MgSO_4$, and the solvent was evaporated. The residue was chromatographed on silica gel eluting with ethyl acetate/hexane (10/90).

[Sal-(*R*)-Bt]. Yield: 10.0%. ^{1}H-NMR (400 MHz, $CDCl_3$): δ/p.p.m. = 10.9 (s, 1H, -OH), 7.85 (d, 1H, *J* = 8 Hz, Ar), 7.45 (t, 1H, *J* = 8 Hz, Ar), 6.97 (d, 1H, *J* = 8 Hz, Ar), 6.88 (t, 1H, *J* = 8 Hz, Ar), 5.08–5.18 (m, 1H, -^{2}CH), 1.64–1.84 (m, 2H, -$^3CH_2$), 1.36 (d, 3H, *J* = 6 Hz, -$^1CH_3$), 0.98 (t, 3H, *J* = 8 Hz, -$^4CH_3$). Elemental analysis: Calculated for $C_{11}H_{14}O_3$: C, 68.02%, H, 7.27%. Measured: C, 68.13%, H, 7.52%.

[Sal-(*S*)-Bt]. Yield: 9.7%. ^{1}H-NMR (400 MHz, $CDCl_3$): δ/p.p.m. = 10.9 (s, 1H, -OH), 7.85 (d, 1H, *J* = 8 Hz, Ar), 7.45 (t, 1H, *J* = 8 Hz, Ar), 6.97 (d, 1H, *J* = 8 Hz, Ar), 6.88 (t, 1H, *J* = 8 Hz, Ar), 5.08–5.18 (m, 1H, -^{2}CH), 1.64–1.84 (m, 2H, -$^3CH_2$), 1.36 (d, 3H, *J* = 6 Hz, -$^1CH_3$), 0.98 (t, 3H, *J* = 8 Hz, -$^4CH_3$). Elemental analysis: Calculated for $C_{11}H_{14}O_3$: C, 68.02%, H, 7.27%. Measured: C, 68.15%, H, 7.49%.

Synthesis of $[Tb_9(sal\text{-}(R/S)\text{-}Bt)_{16}(\mu\text{-}OH)_{10}]^+[NO_3]^-$ ([Tb-(*R/S*)-Bt])

(*R/S*)-2-butyl salicylate (0.20 g, 1.0 mmol) was dissolved in CH_3OH, and Et_3N (0.174 g, 1.72 mmol) was added to this solution with stirring at 40 °C. $Tb(NO_3)_3\cdot 6H_2O$ (0.26 g, 0.58 mmol) in CH_3OH was added dropwise to this solution with further stirring for 20 min.[6,23] A white powder, Tb-(*R/S*)-Bt, was obtained.

[Tb-(*R*)-Bt]. Selected IR (KBr, cm^{-1}): 1680 (-C=O), 2930 (-CH_2-), 2960 (-CH_3). Elemental analysis: Calculated for $C_{176}H_{218}NO_{61}Tb_9$: C, 44.47%, H, 4.62%, N, 0.29%. Measured: C, 44.12%, H, 4.55%, N, <0.30%. Fast atom bombardment–mass spectrometry: *m/z* Calculated for $C_{176}H_{218}O_{58}Tb_9$: [M-NO_3]$^+$, 4691.75; Measured, 4691.79.

[Tb-(*S*)-Bt]. Selected IR (KBr, cm^{-1}): 1680 (-C=O), 2930 (-CH_2-), 2960 (-CH_3). Elemental analysis: Calculated for $C_{176}H_{218}NO_{61}Tb_9$: C, 44.47%, H, 4.62%, N, 0.29%. Measured: C, 44.50%, H, 4.78%, N, 0.31%. Fast atom bombardment–mass spectrometry: *m/z* Calculated for $C_{176}H_{218}O_{58}Tb_9$: [M-NO_3]$^+$, 4691.75; Measured, 4691.76.

Spectral measurements

The electronic absorption and CD spectra of Tb-(*R*)-Bt (2.0×10^{-5} M) and Tb-(*S*)-Bt (2.0×10^{-5} M) were measured in CH_3OH at room temperature. The photoluminescence, CPL spectra, luminescence quantum yields and emission lifetimes (1.0×10^{-4} M) were measured in $CHCl_3$ at room temperature.

Faraday rotation measurements

The Tb(III) clusters (95 mg) obtained were added to $CHCl_3$ (1 ml). Then, the solution (0.2 ml) was added to PMMA (2.8 g) dissolved in $CHCl_3$ (10 ml).[6] PMMA films were prepared on glass substrates using a casting method. The thickness of the PMMA film was ~1.2 mm, and the transmittance was >90% in the 400–800 nm region. The external magnetic field was 15 kOe.

RESULTS AND DISCUSSION

Electronic states and chiroptical properties of the Tb(III) clusters

The Tb(III) clusters Tb-(*R*)-Bt and Tb-(*S*)-Bt were composed of 9 Tb (III) ions bridged by 10 μ-OHs and 16 chiral salicylate ligands. These structures were identified by infrared spectroscopy, fast atom bombardment–mass spectrometry and elemental analysis. X-ray diffraction patterns also demonstrated that the peaks generated by Tb-(*R*)-Bt were consistent with those produced by Tb-(*S*)-Bt (Supplementary Figure S1).

The absorption spectra of the Tb(III) cluster and the ligand are shown in Figure 2a. Intense absorption bands were observed in both Tb-(*R*)-Bt and Tb-(*S*)-Bt at ~340 nm ($\varepsilon_{max}\approx60\,000\ cm^{-1}\ M^{-1}$) because of the π–π^* transition of the salicylate ligands (Figure 2a, red line). The spectrum of the Tb(III) clusters was red shifted and broadened compared with that of the ligands (Figure 2a, black line). This red shift is primarily attributed to destabilization of the highest occupied molecular orbital level as a result of the complexation.[24] The 4f–4f transition of the Tb(III) ions (expected at 488 nm) was not observed because this transition is essentially forbidden by the Laporte rule ($\varepsilon_{max}<1\ cm^{-1}\ M^{-1}$).[25]

These clusters exhibited bisignate CD bands because of the π–π^* transitions of the salicylate ligands (Figure 2b), the signs of which were dependent on the asymmetric centers of the organic ligands. These bisignate spectra were consistent with the absorption maximum peak (335 nm) and shoulder peak (365 nm), respectively, that was attributed to an exciton coupling.[8,26–29] These results indicate that intramolecular interactions might occur between neighboring chiral ligands in the Tb(III) clusters. The band of Tb(III) clusters is not related to CT transition because the Tb(III) ion shows high reduction potential, and its ligand-to-metal charge transfer transition state is located at a higher energy (>60 000 cm^{-1}). Because the electronic state of the Tb(III) ion depends on the coordination geometry formed by the ligands,[25] the intramolecular interactions in the Tb(III) clusters affect the photophysical properties based on the transitions of the Tb (III) ions.

To assess the differences between the electronic states of Tb-(*R*)-Bt and Tb-(*S*)-Bt, we carried out high-resolution photoluminescence measurements. The photoluminescence spectra of the Tb(III) clusters in $CHCl_3$ showed four sharp emission bands in the region of 450–650 nm that were attributed to the $^5D_4\rightarrow{}^7F_J$ ($J=6, 5, 4, 3$) transitions of the Tb(III) ions (Figure 3 and Supplementary Figure S2).[25] In contrast to the absorption spectra, emission bands resulting from the π–π^* transitions of the ligands were not observed. This effect was attributed to the intersystem crossing of the ligand from the excited singlet state to the excited triplet state promoted by the spin orbit coupling of the Tb(III) ions. The crystal field splitting (Stark splitting) of Tb-(*R*)-Bt was consistent with that of Tb-(*S*)-Bt (Figure 3, inset). In time-resolved spectroscopy, the luminescence decays ($^5D_4\rightarrow{}^7F_5$ transition) of the Tb(III) clusters were single exponential (Supplementary Figure S3). These results demonstrate that Tb-(*R*)-Bt and Tb-(*S*)-Bt form mirror image stereoisomers in solution, and these clusters are thus expected to show identical photophysical properties, with the exception of their chiroptical characteristics.

We also performed CPL measurements for these clusters (Figure 4a and b), and the resulting signals were observed to correspond to the transitions of the Tb(III) ions. The observed photophysical properties are summarized in Table 1. Within the experimental error, the clusters had the same luminescence quantum yield, $\Phi_{\pi-\pi^*}$, and luminescence lifetime, τ_{obs}, although their g_{CPL} signs were inverted. The largest g_{CPL}

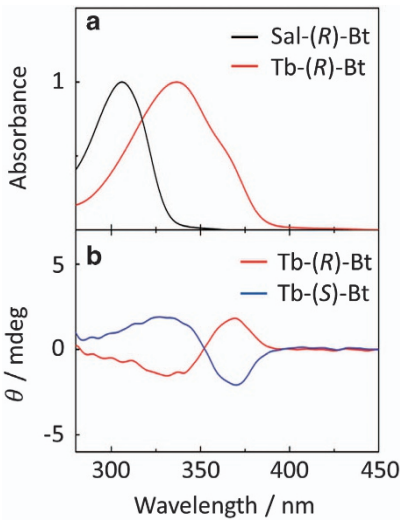

Figure 2 (**a**) Ultraviolet–visible (UV-vis) and (**b**) circular dichroism (CD) spectra of Sal-(*R*)-Bt (black line), Tb-(*R*)-Bt (red line) and Tb-(*S*)-Bt (blue line) in CH_3OH (2.0×10^{-5} M).

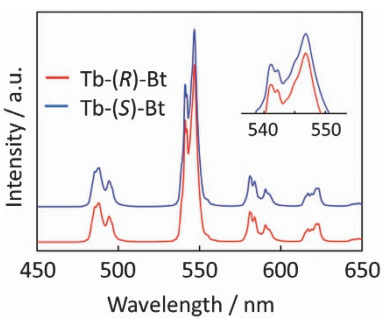

Figure 3 High-resolution photoluminescence (PL) spectra of Tb-(*R*)-Bt (red line) and Tb-(*S*)-Bt (blue line) in $CHCl_3$ (1.0×10^{-4} M).

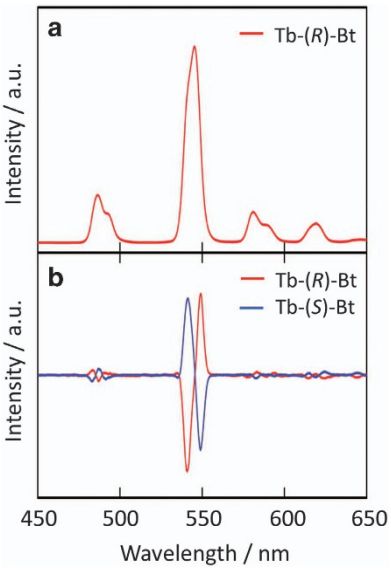

Figure 4 (**a**) Photoluminescence (PL) and (**b**) circularly polarized luminescence (CPL) spectra of Tb-(*R*)-Bt (red line) and Tb-(*S*)-Bt (blue line) in $CHCl_3$ (1.0×10^{-4} M).

Table 1 Luminescence quantum yields ($\Phi_{\pi-\pi^*}$), luminescence lifetimes (τ_{obs}) and dissymmetry factors g_{CPL} of Tb(III) clusters

			g_{CPL}			
Complex	$\Phi_{\pi-\pi^*}$/%	τ_{obs}/ms	$^5D_4\rightarrow{}^7F_6$	$^5D_4\rightarrow{}^7F_5$	$^5D_4\rightarrow{}^7F_4$	$^5D_4\rightarrow{}^7F_3$
Tb-(*R*)-Bt	14	1.3	+0.008	+0.04	+0.005	−0.02
Tb-(*S*)-Bt	15	1.3	−0.01	−0.04	−0.004	+0.03

values were observed at the $^5D_4\rightarrow{}^7F_5$ transitions ($g_{CPL}=\pm0.04$) that were on the same order of magnitude as previously reported for Tb (III) complexes.[12,16,22,24] The large g_{CPL} consequently leads to a large g_{CD},[9] and this is expected to give large transition magnetic dipole moments around the Faraday-active wavelength based on the 4f–4f absorption.

The Faraday effect of the chiral Tb(III) clusters

The wavelength dependence of the Faraday effect was measured using PMMA films containing Tb-(*R*)-Bt or Tb-(*S*)-Bt. The Faraday effect was determined based on the Verdet constant, *V*, as defined in the following equation:[1]

$$V = \theta/Hl \tag{1}$$

where θ, H and l represent the Faraday rotation angle, the external magnetic field and the thickness of the film, respectively. In these experimental trials, we determined the concentration C of the Tb(III) ions in the film using inductively coupled plasma atomic emission spectroscopy. Based on previous work,[6] we subsequently calculated the Verdet constant, *Vc*, normalized by the concentration of Tb(III) ions in the film, as follows:

$$V_C = \theta/HlC. \tag{2}$$

The measured rotation angle consists of a magnetic rotation, θ_F, due to the Faraday effect and a natural rotation, θ_{CD}, due to chirality. To extract θ_{CD} from the total rotational angle, two rotational angles, θ_+ and θ_-, were measured by applying an external magnetic field parallel (+) and antiparallel (−) to the direction of light propagation, respectively (Supplementary Figure S4). These parameters are represented as follows:

$$\theta_+ = \theta_F + \theta_{CD} \tag{3a}$$

$$\theta_- = -\theta_F + \theta_{CD} \tag{3b}$$

The Faraday rotation angle was obtained from Equations (3a and b).

$$\theta = \theta_F = \frac{1}{2}(\theta_+ - \theta_-) \tag{4}$$

The Faraday rotation spectra and the differential spectrum, ΔV_C, are shown in Figure 5a and b. In Figure 5a, negative Faraday rotation angles are observed at ~450 nm. The Verdet constant of the Tb-(*R*)-Bt ($V_{C,max(446\ nm)}=-5.2\times10^{-4}$ deg $Oe^{-1}\,cm^{-1}\,M^{-1}$) was larger than that of the Tb-(*S*)-Bt ($V_{C,\ max(446\ nm)}=-3.4\times10^{-4}$ deg $Oe^{-1}\,cm^{-1}\,M^{-1}$). This result represents the first observation of a Faraday effect that is dependent on the chirality of the clusters.

Generally, the Faraday rotation angle can be expressed as the sum of three terms resulting from three electronic conditions, as follows:[1,30,31]

$$\theta_F \propto f_1 A + f_2\left(B + \frac{C}{kT}\right) \tag{5}$$

Here, f_1 and f_2 are functions that provide an explicit description of the shape of the Faraday effect. The Faraday *A* and *C* terms primarily reflect the degeneracy of the excited and the ground states, respectively, whereas the Faraday *B* term is related to the mixing of the ground and two or more excited states by the magnetic field. In general, the Faraday *C* term is larger than the Faraday *A* and *B* terms.[31] The wavelengths observed in the Faraday effect measurements are associated with several 4f-4f transitions, such as $^7F_6\rightarrow{}^5D_4$ (488 nm), $^7F_6\rightarrow{}^5D_3$ (380 nm)[32] and the broad 4f–5d (below 300 nm)[33] transitions of the Tb(III) ions and the $S_0\rightarrow T_1$ transitions (470 nm) of the ligands.[34] The degenerate ground state is not formed by diamagnetic organic molecules such as the ligands, but rather by the paramagnetic Tb(III) ions depending on the total angular momentum, *J*. In this case, the $^7F_6$ ($J=6$) state of the Tb(III) ions can degenerate into 13 states ($2J+1$). For this reason, the observed signals were primarily due to the transitions of the Tb(III) ions.

The photophysical properties of the Tb(III) ions depend on their coordination geometry. We have previously reported that the Faraday rotation angles of nonanuclear Tb(III) cluster derivatives were changed by altering a substituent in the ligands.[6] This effect results not from changing the electronic state of the ligands, but rather from varying the geometry around the Tb(III) ions of the cluster by using different ester substituents in the ligands.[35] We also demonstrated that the shape of the Stark splitting of Tb-(*R*)-Bt was consistent with that of Tb-(*S*)-Bt based on their geometries (Figure 3 and Supplementary Figure S2), suggesting that difference in the Faraday rotation angle is not derived from configuration interactions between the 4f–4f and 4f–5d transitions. These aspects of the photophysical behavior indicate that the difference between the Faraday rotation angles observed in our experimental work might be attributable to the large transition magnetic dipole moments of Tb-(*R*)-Bt and Tb-(*S*)-Bt. The sign of the transition magnetic dipole moments in the Faraday *B* term inverts depending on the chirality,[1] indicating that this term might be affected by interactions between the 4f–4f ($^7F_6\rightarrow{}^5D_4$) transition and the other 4f–4f transitions such as $^7F_6\rightarrow{}^5D_3$ or the 4f–5d transition.[1] The chirality-induced magneto-optical effect observed in our work is a

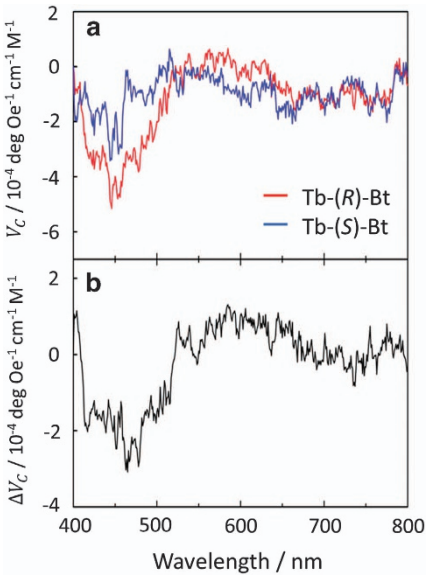

Figure 5 (**a**) The Faraday rotation spectra of Tb-(*R*)-Bt (red line) and Tb-(*S*)-Bt (blue line) and (**b**) the differential spectrum between Tb-(*R*)-Bt and Tb-(*S*)-Bt in poly(methyl methacrylate) (PMMA) films.

different phenomenon from magneto-chiral dichroism (that is, the absorption dependence of a chiral molecule on the direction of a magnetic field).[36–38] Although it is difficult to determine the exact origin of the phenomenon at this stage, this is the first report that Faraday rotation can be affected by chiroptical properties. This result could be a key factor in the design of new materials exhibiting the Faraday effect and may also broaden the field of chiral science.

CONCLUSION

In the present study, we assessed the chiroptical and magneto-optical properties of novel chiral nonanuclear Tb(III) clusters that are composed of 9 Tb(III) ions and 16 chiral 2-butyl salicylate ligands. Faraday effect measurements indicated that the Faraday rotation angles depended on the chirality of the ligands in the Tb(III) clusters. These results provide significant new insight regarding the interrelation between chirality and the Faraday effect. To clarify this mechanism and develop novel magneto-optical materials exhibiting pronounced Faraday rotations, the study of the Faraday effect associated with chiral clusters with large g_{CD} values is now in progress.

CONFLICT OF INTEREST

The authors declare no conflict of interest.

ACKNOWLEDGEMENTS

This work was partly supported by Grants-in-Aid for Scientific Research on Innovative Areas of 'New Polymeric Materials Based on Element-Blocks (no. 2401)' (no. 24102012) of the Ministry of Education, Culture, Sports, Science and Technology (MEXT), Japan. We also thank the Frontier Chemistry Center Akira Suzuki 'Laboratories for Future Creation' Project for their support. We are particularly grateful for the experimental assistance by Professor T Ohkuma and Associate Professor N Arai of Hokkaido University. S Wada was supported by The Ministry of Education, Culture, Sports Science and Technology through Program for Leading Graduate Schools (Hokkaido University 'Ambitious Leader's Program').

1 Schatz, P. N. & McCaffery, A. J. The Faraday effect. *Q. Rev. Chem. Soc.* **23**, 552–584 (1969).
2 Vllora, E. G., Malina, P., Nakamura, M., Shimamura, K., Hatanaka, T., Funaki, A. & Naoe, K. Faraday rotator properties of $\{Tb_3\}[Sc_{1.95}Lu_{0.05}](Al_3)O_{12}$, a highly transparent terbium-garnet for visible-infrared optical isolators. *Appl. Phys. Lett.* **99**, 1–4 (2011).
3 Lin, H., Zhou, S. & Teng, H. Synthesis of $Tb_3Al_5O_{12}$ (TAG) transparent ceramics for potential magneto-optical applications. *Opt. Mater.* **33**, 1833–1836 (2011).
4 Li, W., Zou, K., Lu, M., Peng, B. & Zhao, W. Faraday glasses with a large size and high performance. *Int. J. Appl. Ceram. Technol.* **7**, 369–374 (2010).
5 Yoshida, H., Tsubakimoto, K., Fujimoto, Y., Mikami, K., Fujita, H., Miyanaga, N., Nozawa, H., Yagi, H., Yanagitani, T., Nagata, Y. & Kinoshita, H. Optical properties and Faraday effect of ceramic terbium gallium garnet for a room temperature Faraday rotator. *Opt. Express* **19**, 15181–15187 (2011).
6 Nakanishi, T., Suzuki, Y., Doi, Y., Seki, T., Koizumi, H., Fushimi, K., Fujita, K., Hinatsu, Y., Ito, H., Tanaka, K. & Hasegawa, Y. Enhancement of optical Faraday effect of nonanuclear Tb(III) complexes. *Inorg. Chem.* **53**, 7635–7641 (2014).
7 Riehl, J. P. & Richardson, F. S. Circularly polarized luminescence spectroscopy. *Chem. Rev.* **86**, 1–16 (1986).
8 Harada, N. & Nakanishi, K. *Circular Dichroic Spectroscopy: Exciton Coupling in Organic Stereochemistry* (Tokyo Kagaku Dojin, Tokyo, 1982).
9 Richardson, F. S. Selection rules for lanthanide optical activity. *Inorg. Chem.* **19**, 2806–2812 (1980).
10 Sen, A. C., Chowdhury, M. & Schwartz, R. W. Optical activity of rare earth crystals. Europium oxydiacetate. *J. Chem. Soc. Faraday Trans. 2* **77**, 1293–1300 (1981).
11 Harada, T., Nakano, Y., Fujiki, M., Naito, M., Kawai, T. & Hasegawa, Y. Circularly polarized luminescence of Eu(III) complexes with point- and axis-chiral ligands dependent on coordination structures. *Inorg. Chem.* **48**, 11242–11250 (2009).
12 Yuasa, J., Ohno, T., Miyata, K., Tsumatori, H., Hasegawa, Y. & Kawai, T. Noncovalent ligand-to-ligand interactions alter sense of optical chirality in luminescent tris(*β*-diketonate) lanthanide(III) complexes containing a chiral bis(oxazolinyl) pyridine ligand. *J. Am. Chem. Soc.* **133**, 9892–9902 (2011).
13 Lunkley, J. L., Shirotani, D., Yamanari, K., Kaizaki, S. & Muller, G. Chiroptical spectra of a series of tetrakis((+)-3-heptafluorobutylyrylcamphorato)lanthanide (III) with an encapsulated alkali metal ion: circularly polarized luminescence and absolute chiral structures for the Eu(III) and Sm(III) complexes. *Inorg. Chem.* **50**, 12724–12732 (2011).
14 Bonsall, S. D., Houcheime, M., Straus, D. A & Muller, G. Optical isomers of N,N'-bis(1-phenylethyl)-2,6-pyridinedicarboxamide coordinated to europium(III) ions as reliable circularly polarized luminescence calibration standards. *Chem. Commun.* **35**, 3676–3678 (2007).
15 Seitz, M., Do, K., Ingram, A. J., Moore, E. G., Muller, G. & Raymond, K. N. Circularly polarized luminescence in enantiopure europium and terbium complexes with modular, all-oxygen donor ligands. *Inorg. Chem.* **48**, 8469–8479 (2009).
16 Seitz, M., Moore, E. G., Ingram, A. J., Muller, G. & Raymond, K. N. Enantiopure, octadentate ligands as sensitizers for europium and terbium circularly polarized luminescence in aqueous solution. *J. Am. Chem. Soc.* **129**, 15468–15470 (2007).
17 Bozoklu, G., Gateau, C., Imbert, D., Pécaut, J., Robeyns, K., Filinchuk, Y., Memon, F., Muller, G. & Mazzanti, M. Metal-controlled diastereoselective self-assembly and circularly polarized luminescence of a chiral heptanuclear europium wheel. *J. Am. Chem. Soc.* **134**, 8372–8375 (2012).
18 Mamula, O., Lama, M., Telfer, S. G., Nakamura, A., Kuroda, R., Stoeckli-Evans, H. & Scopelitti, R. A trinuclear Eu(III) array within a diastereoselectively self-assembled helix formed by chiral bipyridine-carboxylate ligands. *Angew. Chem. Int. Ed.* **44**, 2527–2531 (2005).
19 Lama, M., Mamula, O., Kottas, G. S., Rizzo, F., Cola, L. D., Nakamura, A., Kuroda, R & Stoeckli-Evans, H. Lanthanide class of a trinuclear enantiopure helical architecture containing chiral ligands: Synthesis, structure, and properties. *Chem. Eur. J.* **13**, 7358–7373 (2007).
20 Stomeo, F., Lincheneau, C., Leonard, J. P., O'Brien, J. E., Peacock, R. D., McCoy, C. P. & Gunnlaugsson, T. Metal-directed synthesis of enantiomerially pure dimetallic lanthanide luminescent triple-stranded helicates. *J. Am. Chem. Soc.* **131**, 9636–9637 (2009).
21 Gregoliński, J., Starynowicz, P., Hua, K. T., Lunkley, J. L., Muller, G. & Lisowski, J. Helical lanthanide (III) complexes with chiral nonaaza macrocycle. *J. Am. Chem. Soc.* **130**, 17761–17773 (2008).
22 Petoud, S., Muller, G., Moore, E. G., Xu, J., Sokolnicki, J., Riehl, J. P., Le, U. N., Cohen, S. M. & Raymond, K. N. Brilliant Sm, Eu, Tb, and Dy chiral lanthanide complexes with strong circularly polarized luminescence. *J. Am. Chem. Soc.* **129**, 77–83 (2007).
23 Manseki, K. & Yanagida, S. Effective and efficient photoluminescence of salicylate-ligating terbium(III) clusters stabilized by multiple phenyl-phenyl interactions. *Chem. Commun.* **12**, 1242–1244 (2007).
24 Wada, S., Kitagawa, Y., Nakanishi, T., Fushimi, K. & Hasegawa, Y. Chiroptical properties of nonanuclear Tb(III) clusters with chiral champhor derivative ligands. *e-J. Surf. Sci. Nanotech.* **13**, 31–34 (2015).
25 Eliseeva, S. V. & Bünzli, J.-C. G. Lanthanide luminescence for functional materials and bio-sciences. *Chem. Soc. Rev.* **39**, 189–227 (2010).

26 Bobba, G., Bretonnière, Y., Frias, J.-C. & Parker, D. Enantiopure lanthanide complexes incorporating a tetraazatriphenylene sensitiser and three naphthyl groups: exciton coupling, intramolecular energy transfer, efficient singlet oxygen formation and perturbation by DNA binding. *Org. Biomol. Chem.* **1**, 1870–1872 (2003).
27 Dickins, R. S., Howard, J. A. K., Moloney, J. M., Parker, D., Peacock, R. D. & Siligardi, G. Strong exciton coupling and circularly polarised luminescence in rigid complexes of chiral macrocyclic tetranaphthylamides. *Chem. Commun.* 1747–1748 (1998).
28 Kotova, O., Blasco, S., Twamley, B., O'brien, J. E., Peacock, R. D., Kitchen, J. A., Martínez-Calvo, M. & Gunnlaugsson, T. The application of chiroptical spectroscopy (circular dichroism) in quantifying binding events in lanthanide directed synthesis of chiral luminescent self-assembly structures. *Chem. Sci.* **6**, 457–471 (2015).
29 Dickins, R. S., Howard, J. A. K., Maupin, C. L., Moloney, J. M., Parker, D., Peacock, R. D., Riehl, J. P. & Siligardi, G. Ground and excited state chiroptical properties of enantiopure macrocyclic tetranaphthyl lanthanide complexes: controlled modulation of the frequency and polarisation of emitted light. *New J. Chem.* **22**, 891–899 (1998).
30 Djerassi, C., Bunnenberg, E. & Elder, D. L. Organic chemical applications of magnetic circular dichroism. *Pure Appl. Chem.* **25**, 57–90 (1971).
31 McCaffery, A. J. New application for magnetic circular dichroism. *Nature Phys. Sci.* **232**, 137–140 (1971).
32 Carnall, W. T., Hessler, J. P. & Wagner, F. J. Transition probabilities in the absorption and fluorescence spectra of lanthanides in molten lithium nitrate -potassium nitrate eutectic. *J. Phys. Chem.* **82**, 2152–2158 (1978).
33 Miyamoto, K., Isai, K., Suwa, M. & Watarai, H. Effective transition probability for the Faraday effect of lanthanide (III) ion solutions. *J. Am. Chem. Soc.* **131**, 6328–6329 (2009).
34 Omagari, S., Nakanishi, T., Seki, T., Kitagawa, Y., Takahata, Y., Fushimi, K., Ito, H. & Hasegawa, Y. Effective photosensitized energy transfer of nonanuclear terbium cluster using methyl salicylate derivatives. *J. Phys Chem. A* **119**, 1943–1947 (2015).
35 Fluyt, L., Verhoeven, P., Lambaerts, H., Binnemans, K. & Görller-Walrand, C. Magnetic circular dichroism for generating crystal wave functions. *J. Alloys Compd.* **208**, 51–54 (1994).
36 Kitagawa, Y., Segawa, H. & Ishii, K. Magneto-chiral dichroism of organic compounds. *Angew. Chem. Int. Ed.* **50**, 9133–9136 (2011).
37 Rikken, G. L. J. A. & Raupach, E. Observation of magneto-chiral dichroism. *Nature* **390**, 493–494 (1997).
38 Rikken, G. L. J. A. & Raupach, E. Enantioselective magnetochiral photochemistry. *Nature* **405**, 932–935 (2000).

Supplementary Information accompanies the paper on the NPG Asia Materials website (http://www.nature.com/am)